THE KOREAN JOURNAL OF QUATERNARY RESEARCH Vol. 19, No. 2 p. 45-49 (December. 2005)

High-resolution Simulation of the Asian Monsoon at 6000 Years BP

Seong-Joong Kim[1*], Thomas J. Crowley[2], Bang-Yong Lee[1] and Bong-Chool Suk[3]

[1]*Korea Polar Research Institute*

[2]*Division of Earth and Ocean Sciences, Duke University Durham, USA*

[3]*Korea Ocean Research & Development Institute, Korea*

1. Introduction

The most active convection in Asian monsoon areas leads to a transfer of heat and moisture to adjacent lands and largely influences the climate, culture, and economy in those areas (Fein and Stephens, 1987; Ding, 1994; Webster et al., 1998). There are two phases of the Asian monsoon: wet and dry. The wet phase refers to the rainy season during which warm, moist winds blow to land from tropical oceans, while the dry phase refers to a dry season during which cold and dry air blows from the continents. The inter-annual fluctuation of the monsoon is known to largely influence agriculture. A weak monsoon year (i.e. significantly less total rainfall than normal) is generally associated with low crop yields, while a strong monsoon usually produces abundant crops though too much rain leads to devastating floods.

The increase in fossil fuel consumption and a large-scale de-forestation have led to a dramatic increase in greenhouse gases and eventually an increase in global surface temperature. Some numerical experiments have shown that the global warming may lead to a large-scale change in atmospheric circulation including that of the Asian monsoon in the near future (e.g., Douville et al., 2000; Hu et al., 2000). For a better prediction of future climate change, numerical models' predictability must be tested. The mid-Holocene at 6000 years before present (6kBP) serves the best opportunity to test a model's skill in prediction, including monsoon circulation, because the mid-Holocene was slightly warmer than present and relatively abundant proxy records are available.

During the mid-Holocene at 6000 years before present (6kBP) the summer insolation was about 7% (30 W m^{-2}) higher than present at 65°N, whereas it was reduced by 3.5% (15 W m^{-2}) at 65°S. Temporal variations of solar insolation largely depend on the variation in orbital parameters, eccentricity, obliquity, and precession. At 6kBP, obliquity was larger (24.1°) than at present (23.44°) and longitude of perihelion differed by about 100°. In this study, we revisited the simulation of the change in the Asian monsoon 6kBP using attempt to address the limits of coarse grid modelling by inga fine resolution atmospheric general circulation model (AGCM) and compare with the paleoclimate proxy data and other model results.

2. Model description and experiments

The simulations were performed with the Community Climate Model version 3 (CCM3) atmospheric general circulation model at T170 truncation. The transform grid has 512 x 256 cells, with a typical grid size of about 75 km with 18 vertical levels. We used a model version known as "CCM3.10.11 with 3.6.6 physics." This has identical physics to CCM3.6.6, but the computational aspects of the model have been re-written to allow more reliable and efficient operation on massively parallel computers as illustrated in Duffy et al.(2003). Important

physical processes are described in detail by Kiehl et al. (1998 a, b). The CCM3 includes a comprehensive model of land surface processes known as the NCAR Land Surface Model (LSM; Bonan, 1998). Some relevant properties of our simulations are summarized in Duffy et al. (2003).

The results of two experiments are analyzed. The modern climate simulation is forced by prescribed, climatologically-averaged, monthly sea-surface temperatures (SSTs) and sea ice distributions provided by NCAR, a specified CO_2 concentration of 355 ppm, and present land mask and topography. This experiment is referred to as "MOD." The mid-Holocene experiment, called "HOL," has identical conditions to the MOD experiment except for orbital parameters set for 6kBP as illustrated in Fig. 2. Ice core records showed that the atmospheric CO_2 concentration is observed to be about 270 ppm at 6kBP (Indermühle et al., 1999; Raynaud et al., 2000). This value is almost similar to that of the pre-industrial period (280 ppm) and the impact of the change in atmospheric CO_2 concentration between the mid-Holocene and the pre-industrial period on the climate change seems to be negligible. In the HOL experiment SST is specified as the present climatological SST. This is because the change in SST between the two periods appears to be relatively small (Ruddiman and Mix, 1993) and previous models studies also applied the present SSTs for the mid-Holocene experiment (e.g., de Noblet et al., 1996; Hewitt and Mitchell, 1996).

3. Results

In winter, the reduction in short wave radiations leads to an overall cooling over almost all of the Asian land masses surface temperature decreases overall during the mid-Holocene in comparison to present. The winter surface cooling is especially pronounced in India, the Arabia peninsula, South Asia, and northern Africa, where the surface temperature decreases by more than 2°C. In some regions such as northern China a warming by 2°C is simulated. This warming is partially associated with the increase in shortwave radiation. In areas such as warming is simulated. In summer, the short wave radiation increases in most of the Asian areas and this increase leads to the surface warming at 6kBP by 2~4°C. The surface warming is particularly pronounced in the western Mongolia where the surface warming reaches by more than 4°C. In the southern part of Asia, the slight summer cooling is simulated. This cooling is presumably associated with the surrounding seas.

The change in surface temperature presumably leads to the change in surface pressure system. In winter at 6kBP, the MSLP increases over Tibetan Plateau, India, Saudi Arabia, and northern Africa where the reduction in surface temperature is relatively large. The anticyclone associated with the Siberian high became slightly stronger in the southern part of Himalaya, while it becomes weaker in the northern part of Himalaya. In summer, overall increase in the surface temperature leads to the reduction in the MSLP in Asia. The deepening of the MSLP is especially pronounced over Tibetan Plateau, which is associated with the marked increase in the surface temperature.

The spatial distribution of MSLP implies the variation of surface winds. In winter, surface winds blow from the continent to the adjacent seas due to the anticyclone developed around Siberia. The anticyclone leads to strong northwesterly winds in eastern Asia and northeasterly winds in the Arabian Sea. In summer, the winds become reversed, blowing from the ocean to the continent. The most distinctive landward wind is the strong southwesterly Somali jet blowing from the Arabian Sea to western India. This landward wind pattern is due to the cyclonic low pressure system over Himalaya.

In the mid-Holocene, the Siberian high-pressure slightly increases and is shifted slightly to the south in winter. This leads to an enhancement and southward displacement of the southeasterly winds in the Indian Ocean. In the North Pacific, the northwesterly becomes slightly weaker associated with the weakening of the high-pressure system in that region. In summer, deeper surface pressure leads to an increase in landward winds,

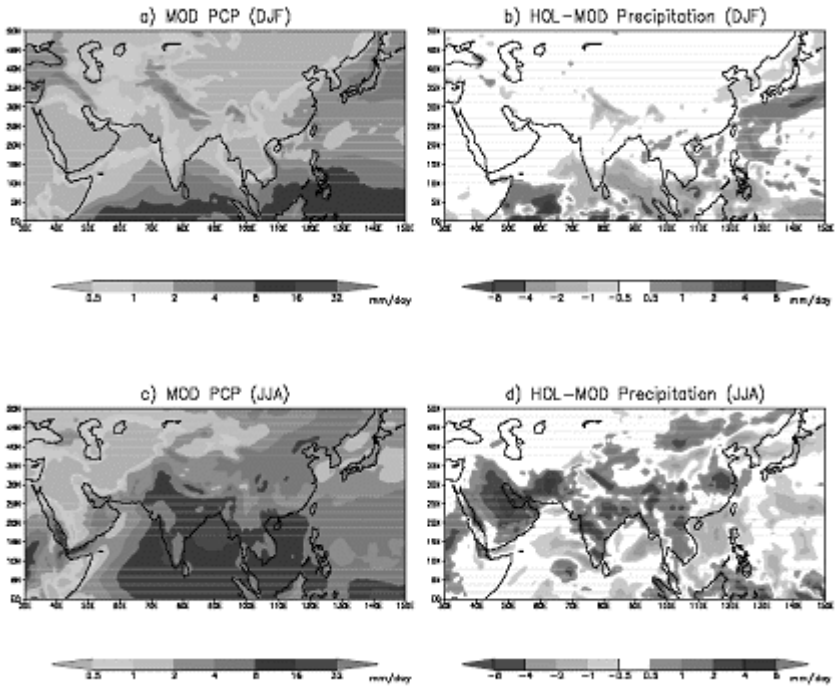

a) mean, b) change and in summer c) mean, d) change. Units are mm d^{-1}.

Fig. 1 Geographic distribution of the change in precipitation in winter

especially the southwesterly winds in the Arabian Sea.

The spatial wind pattern is closely linked to the distribution of the precipitation. Fig. 1 shows the winter and summer precipitation in the MOD experiment and its changes from the HOL experiment. In the MOD experiment, precipitation is low in northern and eastern China, Mongolia, and Saudi Arabia in winter as would be expected from the distribution of the winds. As mentioned above, in winter, surface winds blow from the continent leading to the extremely low precipitation inside the continent. In summer, on the other hand, precipitation is overall large in most Asian regions, especially in Bay of Bengal, India, and South Asia by more than 4 mm per day. The high precipitation in those regions is due to the strong southwest wind in the Arabian Sea which transfers moisture to the adjacent lands.

The change in precipitation at 6kBP appears to be associated with the change in wind fields. In winter, the slight increase in seaward winds leads to a slight reduction in precipitation in the northern and southern part of India. Otherwise there is little change in precipitation over most of the land areas. The little change in winter precipitation may be due to little moisture source over central Asia. There is a large reduction in precipitation over the central and eastern part of the Indian Ocean and western Pacific. In summer, on the other hand, a large increase in precipitation is found over the Arabia Peninsula, India, South Asia. The increase in summer precipitation at 6kBP is presumably due to the increases in the southwesterly wind in the Arabian Sea toward India.

Fig. 2 compares the simulated annual mean change in hydrological budget (precipitation minus evaporation) to that inferred from the change in lake level. In the mid-Holocene, the South Asia including the Arabia and Indo-China peninsula is overall wetter. This result is

broadly consistent with the lake level data, which shows that it was wetter in the north-eastern part of Africa,

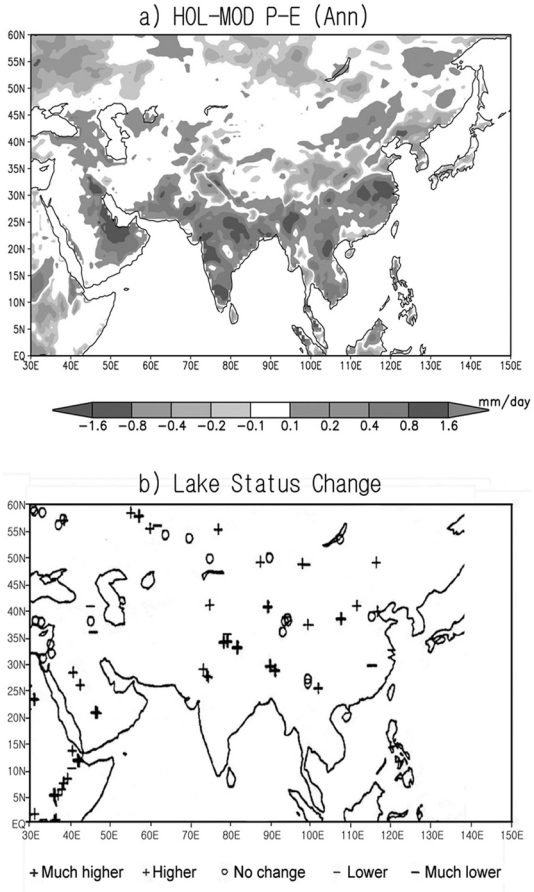

Fig. 2 Geographic distribution of the change in annual-mean. a) precipitation minus evaporation, b) hydrological budget estimated from lake status (adapted from *de Noblet et al.*, 1996). Units are mm d^{-1}.

Saudi Arabia, northern India, northern and southern part of China, and around Mongolia. A similar result is obtained by other lake level data (Yu and Harrison, 1996; Kohfeld and Harrison, 2000).

Overall, at 6kBP there is little change in precipitation over Asia in winter, whereas precipitation increases in the southern part of Asia due to the enhanced southwesterly wind in the Arabian Sea by the stronger low-pressure over the Tibetan Plateau associated with the marked increase in surface temperature.

4. Conclusions

In conclusion, the high resolution model simulation reproduces climate features for the mid-Holocene at 6kBP in comparison to the paleoclimate proxy estimates and shows the enhanced summer monsoon.

Acknowledgements This study was supported by projects of Studies on the Arctic Environmental Characteristics (PE05007) and the evolution of Asian monsoon of the Korea Ocean Research and Development Institute (PG04001).

References

Bonan, G. 1998, The land surface climatology of the NCAR Land Surface Model coupled to the NCAR Community Climate Model, J. Clim., 11, 1307-1326.

de Noblet, N., P. Braconnot, S. Joussaume, and V. Masson. 1996, Sensitivity of simulated Asian and African summer monsoons to orbitally induced variations in insolation 126, 115, 6 kBP, Clim. Dyn., 12, 589-603.

Ding, Y. 1994, Monsoons over china, 419 pp., Kluwer Academy Publishers, London.

Douville, H., J.-F. Royer, J. Polcher, P. Cox, N. Gedney, D. B. Stephenson, and P. J. Valdes. 2000, Impact of CO_2 doubling on the Asian summer monsoon: Robust versus model-dependent responses, J. Meteorol. Soc. Jpn., 78, 421-439.

Duffy, P. B., B. Govindasamy, J. P. Iorio, J. Milovich, K. R. Sperber, K. E. Taylor, M. F. Wehner, and S. L. Thompson. 2003, High-resolution simulations of global climate, part 1: present climate, Clim. Dyn., 21, 371-390.

Fein J. S., and P. L. Stephens. 1987, Monsoons, 632 pp., John Wiley and Sons, U.S.A.

Hewitt, C. D., and J. F. B. Mitchell. 1996, GCM simulations of the climate of 6 kyr BP: Mean changes and interdecadal variability, J. Clim., 9, 3505-3529.

Hu, Z.-Z., L. Bengtsson, and K. Arpe. 2000, Impactof global warming on the Asian winter monsoon in a coupled GCM, J. Geophys. Res., 105, 4607-4624.

Indermühle, A., T. F. Stocker, F. Joos, H. Fischer, H. J. Smith, M. Wahlen, B. Deck, D. Mastroianni, J. Tschumi, T. Blunier, R. Meyer, and B. Stauffer. 1999, Holocene carbon-cycle dynamics based on CO_2 trapped in ice at Taylor Dome, Antarctica, Nature, 398, 121-126.

Kiehl, J. T., J. J. Hack, B. G. Bonan, B. A. Boville, D. L. Williamson, and P. Rasch. 1998a, The National Center for Atmospheric Research Community Climate Model: CCM3, J. Clim., 11, 1131-1149.

Kiehl, J. T., J. J. Hack, and J. Hurrell. 1998b, The energy budget of the NCAR Community Climate Model: CCM3, J. Clim., 11, 1151-1178.

Kohfeld, K. E., and S. P. Harrison. 2000, How well can we simulate past climates? Evaluating the models using global paleoenvironmental datasets, Quat. Sci. Rev., 19, 321-346.

Raynaud, D., J.-M. Barnola, J. Chappellaz, T. Blunier, A. Indermühle, and B. Stauffer. 2000, The ice record of greenhouse gases: a view in the context of future changes, Quat. Sci. Rev., 19, 9-17.

Ruddiman, W. F., and A. C. Mix. 1993, The north and equatorial Atlantic at 9000 and 6000 yr BP, in: Global climates since the Last Glacial Maximum. edited by H. E. J. Wright, J. E. Kutzbach, T. Webb III, W. F. Ruddiman, F. A. Street-Perrott, and P. J. Bartlein, pp. 94-124, Univ. Minnesota Press, Minneapolis.

Yu, G., and S. P. Harrison. 1996, An evaluation of the simulated water balance of Eurasia and northern Africa at 6000 yr BP using lake status data, Clim. Dyn., 12, 723-735.

Webster, P. J., V. O. Magana, T. N. Palmer, J. Shukla, R. A. Tomas, M. Yanai, and T. Yasunari. 1998, Monsoons: Processes, predictability, and the prospects for prediction, J. Geophys. Res., 103, 14451-14510.